SUPPLEMENTAL INFORMATION

List of Supplemental Tables, Figures, and Movies

Table S1. (related to Figure 1)

Egfr^{Em} mice were born at the expected Mendelian ratio in a C57BL/6 or a CD1 background.

***Egfr*$^{Em/+}$ x wild-type (C57BL/6)**

Genotype	wild-type	*Egfr*$^{Em/+}$	*Egfr*$^{Em/Em}$
Adult #	48	47	0
Relative ratio	1	0.98	0
Expected ratio	1	1	0

***Egfr*$^{Em/+}$ x *Egfr*$^{Em/+}$ (C57BL/6)**

Genotype	wild-type	*Egfr*$^{Em/+}$	*Egfr*$^{Em/Em}$
Adult #	13	24	12
Relative ratio	1	1.85	0.93
Expected ratio	1	2	1

***Egfr*$^{Em/+}$ x wild-type (CD1)**

Genotype	wild-type	*Egfr*$^{Em/+}$	*Egfr*$^{Em/Em}$
Adult #	60	63	0
Relative ratio	1	1.05	0
Expected ratio	1	1	0

***Egfr*$^{Em/+}$ x *Egfr*$^{Em/+}$ (CD1)**

Genotype	wild-type	*Egfr*$^{Em/+}$	*Egfr*$^{Em/Em}$
Adult #	21	50	22
Relative ratio	1	2.38	1.05
Expected ratio	1	2	1

Figure S1 (related to Figure 1)

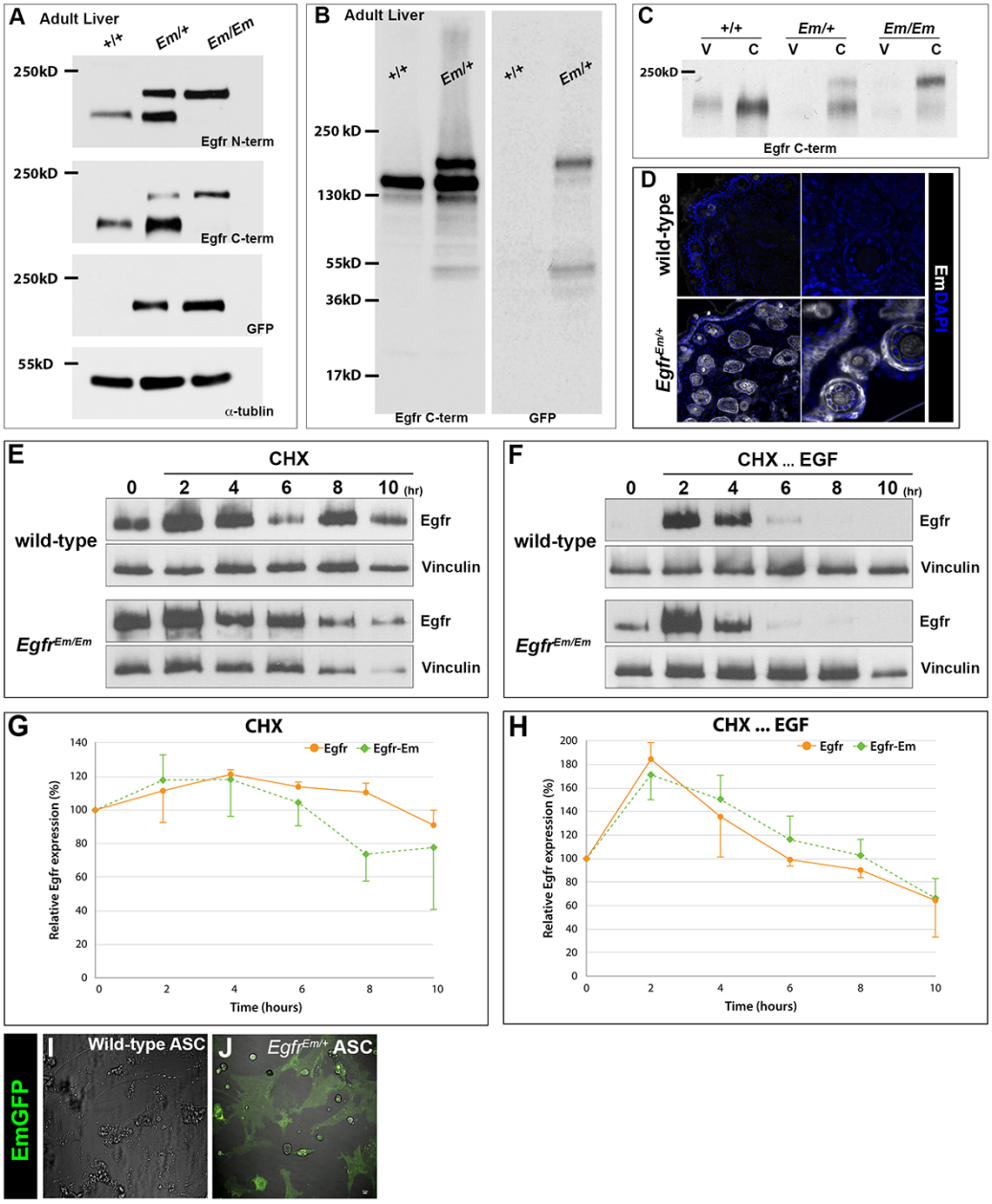

Figure S1 (related to Figure 1)

Characterization of Egfr-Em fusion protein. (A) Immunoblot analysis of adult liver from various genotypes using antibodies against N-terminus Egfr, C-terminus Egfr, and GFP. **(B)** Immunoblot analysis of adult liver of shown genotypes showed no detectable free cleaved GFP from Egfr-Em fusion protein (expected 27kD). **(C)** Immunoblot analysis of adult intestinal villus (V) and crypt (C) fractions of various genotypes showing enriched Egfr (or Egfr-Em) in the crypts. **(D)** Direct fluorescence of adult mouse tail cryosections showed fluorescence detection was associated with the *Egfr*^{Em} allele. **(E-H)** Cycloheximide chase assays on primary culture of adipose-derived mesenchymal stem cells (ASC) from wild-type and *Egfr*$^{Em/Em}$ mice. Cycloheximide (30 μg/ml) was added at time 0 minute alone (E,G) or with EGF (50 ng/ml) added 30 minutes after (F,H). Egfr and Vinculin levels were monitored over time. Representative blots (E,F) and densitometric quantification (G,H) are shown. Data represent percentage of Egfr intensity of three independent experiments (mean ± SEM) compared with that at time 0 minute. No significant difference was found. **(I,J)** Egfr-Em direct fluorescence was detected in ASC from *Egfr*$^{Em/+}$ (J) but not those from wild-type mice (I).

Figure S2 (related to Figure 2)

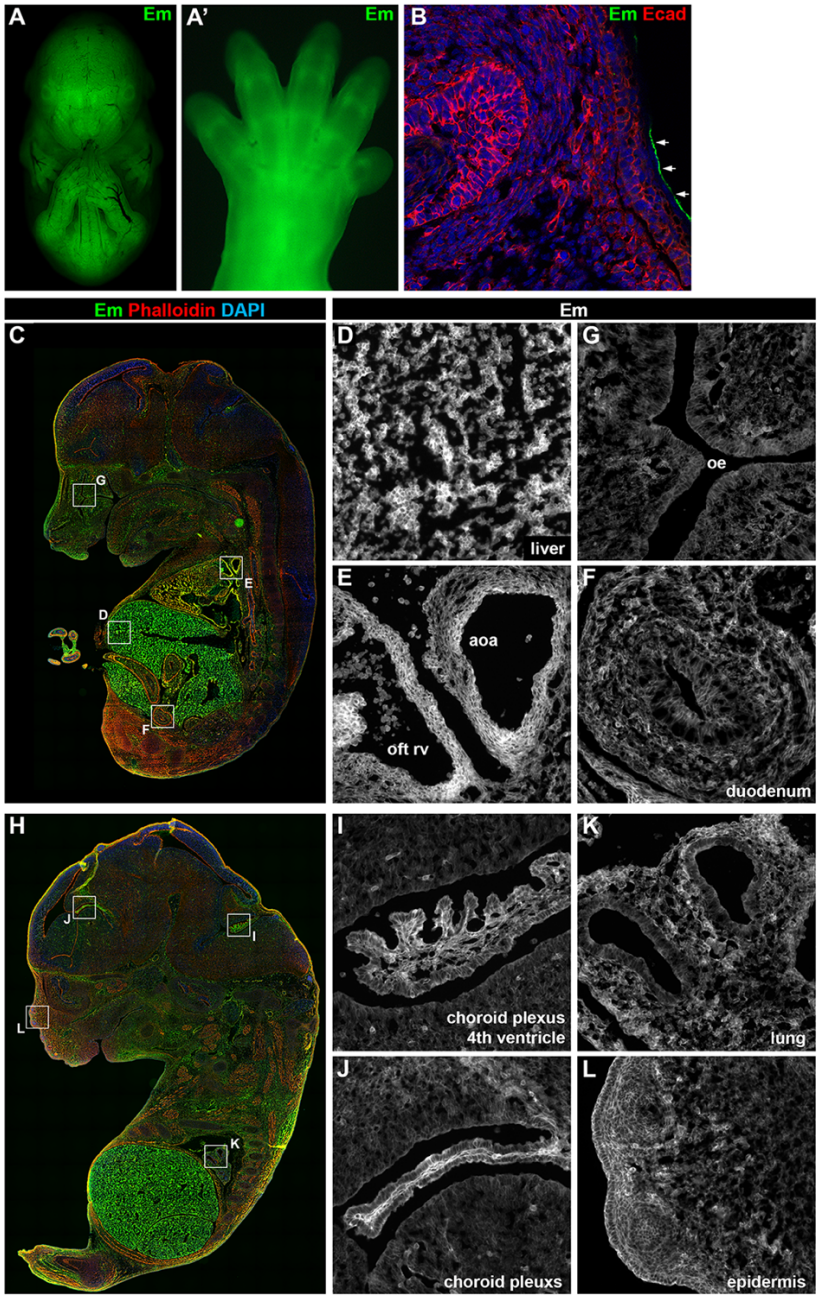

Figure S2 (related to Figure 2)

Egfr-Em expression in E14.5 embryo. (A) Wholemount direct fluorescence of an 14.5 embryo, frontal view. **(A')** Egfr-Em was enriched in the interphalageal zones of the limb. **(B)** Whisker follicle cells and epidermal cells from a wild-type embryo showed no Egfr-Em immunodetection but autofluorescence in the keratinized epithelium (arrows). **(C-F)** Overview of a sagittal section. Egfr-Em was detected in the liver (D), aorta arch (aoa) and outflow tract of the right ventricle (oft rv in E), olfactory epithelium (oe in G), and the duodenum (F). **(H-L)** Overview of another sagittal section of the embryo with enriched expression detected in choroid plexus (I, J), in the bronchus of the lung (K), and in the epidermis (L).

Figure S3 (related to Figure 3)

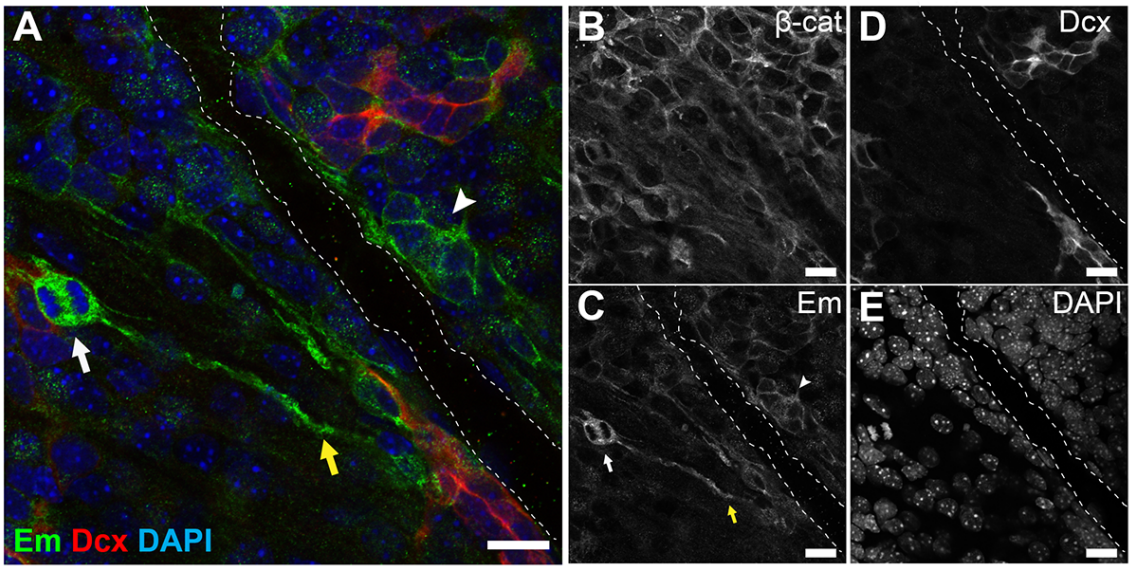

Figure S3 (related to Figure 3)

Egfr-Em-expressing cells are likely aB1 cells and C cells. Confocal images for a V-SVZ wholemount immunostaining for Egfr-Em, DCX, β-catenin and DAPI. (**A**) A merged image for Egfr-Em, DCX, and DAPI channels. (**B-E**) Single channel images for β-catenin to visualize ventricular ependymal cells (B), for Egfr-Em (C), for DCX to label neuroblasts (D), and for DAPI to label nuclei (E). White arrows in (A,C) denote a putative aB1 cell in the process of division, which is located beneath the ependymal structure. Yellow arrows (A,C) denote the neuronal projection of the aB1 cell. White arrowhead (A,C) denote Egfr-Em-expressing DCX-negative transit-amplifying cells. Dashed lines (A,C-E) denote the vessel. Scale bars, 20 μm.

Figure S4 (related to Figure 4)

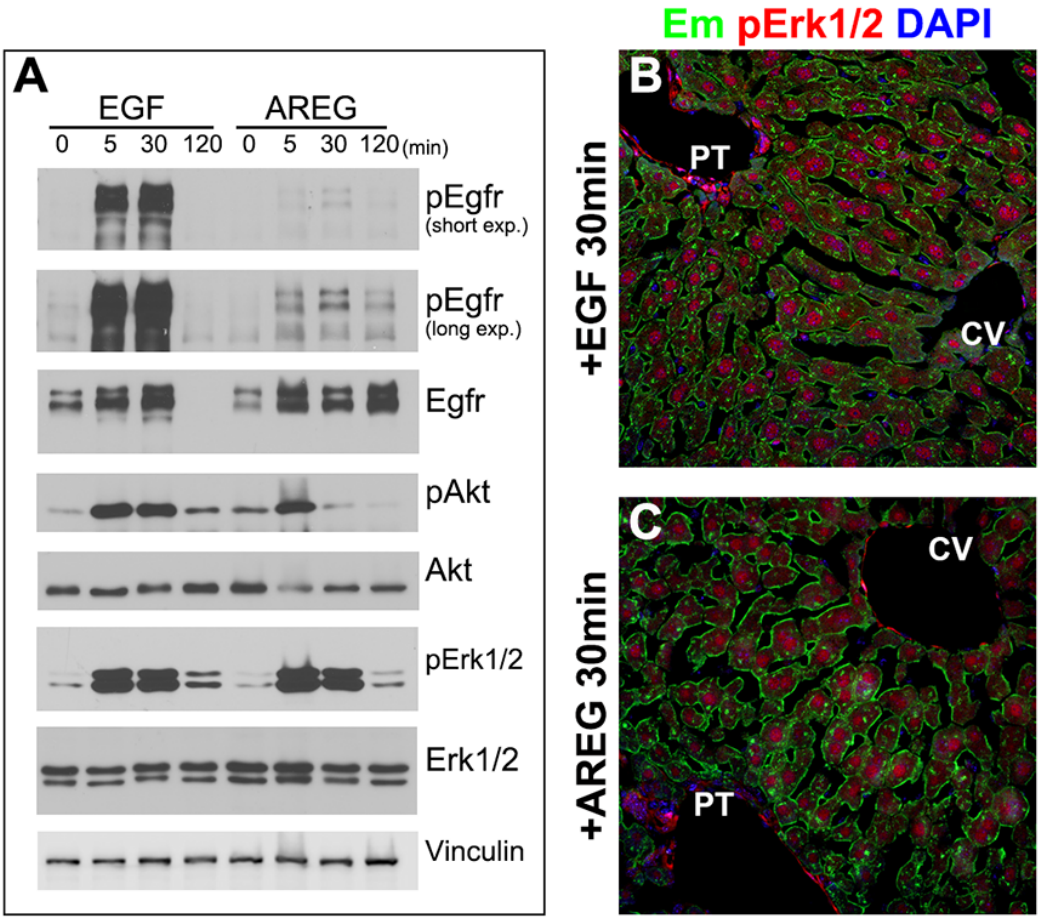

Figure S4 (related to Figure 4)

Activation of Egfr, Egfr-Em and its downstream signaling in the liver by EGF and AREG administration. *Egfr*$^{Em/+}$ mice were injected with EGF (1 μg per gram body weight) or AREG (1.87 μg per gram body weight) intraperitoneally and signaling responses in the liver were monitored over time. (**A**) Immunoblot analysis showed a stronger response in phosphorylation of Egfr and Egfr-Em by EGF injection compared to that by AREG injection. Comparable levels of pAkt and pErk1/2 were detected with EGF and AREG administration. (**B,C**) Upon EGF or AREG treatment, pErk1/2 is present in the nuclei and cytoplasm at 30 minutes. At this time, no obvious difference in the distribution of pErk1/2 was found between the portal tract (PT) and central vein (CV).

Figure S5 (related to Figure 5)

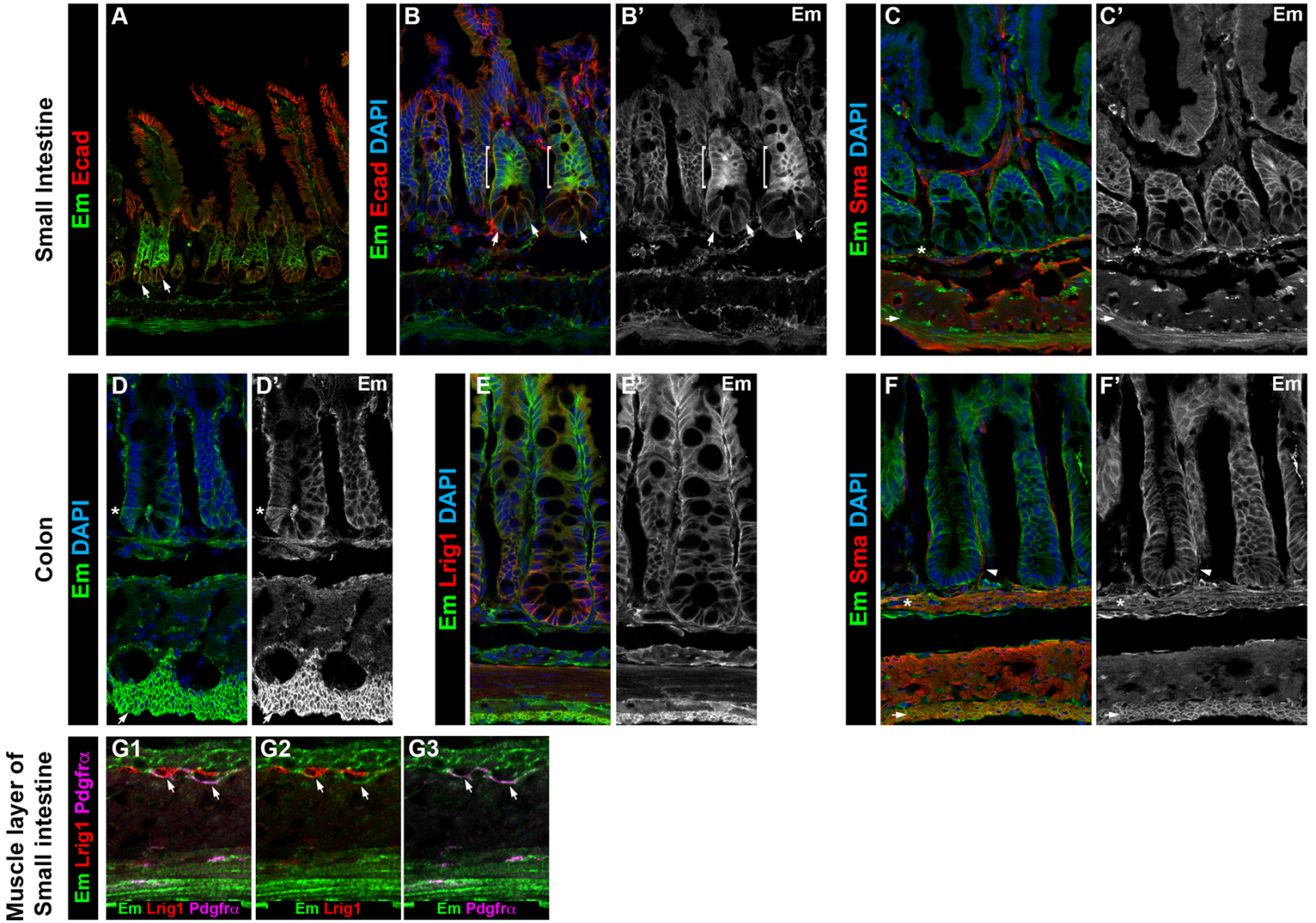

Figure S5 (related to Figure 5)

Egfr-Em expression in small intestine and colon. (A) Overview of Egfr-Em expression in the small intestine showing enriched expression in stem/progenitor cells. Note the two crypts (arrows) with higher Egfr-Em expression compared to the neighboring crypts. **(B,B')** Higher power view of intestinal crypts with heightened Egfr-Em expression in stem/progenitor cells (arrows and brackets). **(C,C')** Egfr-Em co-expressed with SMA in the outer longitudinal muscle (arrows) and muscularis mucosa layer (asterisks) of small intestine. **(D,D')** In colon, Egfr-Em was detected in the membrane throughout the crypts. Asterisks denote cytoplasmic distribution of Egfr-Em in a small number cells at the crypt base. Note the high expression in the longitudinal muscle (arrows). **(E,E')** Egfr-Em co-expresses with Lrig1 in colonic crypts. **(F,F')** In colon, Egfr-Em co-expresses with SMA in longitudinal muscle (arrows), mucosa layer (asterisks) but not in pericryptal fibroblasts (arrowheads). **(G)** Egfr-Em and Pdgfrα co-expression was detected in the fibroblast-like cells (arrows) adjacent to the Lrig1-expressing ICCs in the small intestine.

Figure S6 (related to Figure 6)

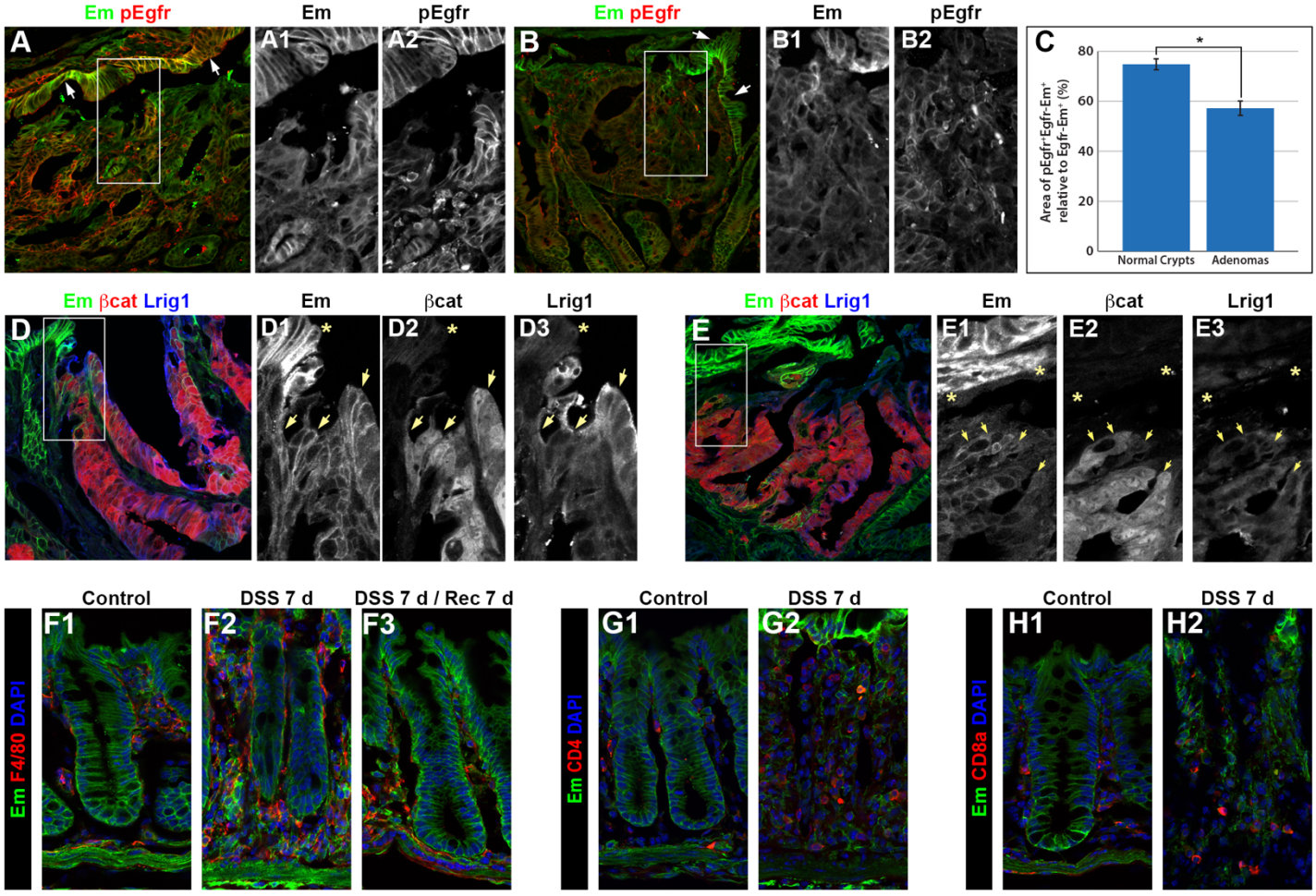

Figure S6 (related to Figure 6)

Egfr-Em expression in small intestinal tumors and in DSS-treated colon. (A,B) Egfr-Em and pEgfr showed heterogeneous staining in small intestinal tumors in *Lrig1*$^{CreER/+}$;*Apc*$^{fl/+}$;*Egfr*$^{Em/+}$ mice. The rim of epithelium surrounding the adenoma showed higher Egfr-Em expression (arrows in A,B). Egfr-Em and pEgfr expression did not directly correlate with each other (A1, A2, B1, B2). **(C)** Proportion of Egfr-Em-pEgfr co-expression relative to pEgfr expression in normal crypts (n=68) and in independent adenomas (n=21). $p<0.05$. **(D,E)** Egfr-Em expression was negatively associated with β-catenin and Lrig1 expression. Lower Egfr-Em expression (D1, E1) was associated with higher cytoplasmic β-catenin expression and higher Lrig1 expression (arrows in D1-3, E1-3). **(F)** In *Egfr*$^{Em/+}$ control colon, Egfr-Em was detected throughout the membrane of the colonic crypts, and weaker Egfr-Em fluorescence was detected in a small number of F4/80-expressing macrophages in the stroma. (F1). After DSS treatment for 7 days, increased numbers of F4/80 cells expressing higher level of Egfr-Em were found in the stroma. F4/80^{-}Egfr-Em^{HI} cells were also found (F2). After 7 days of DSS treatment, followed by another 7 days of recovery, epithelial structures and Egfr-Em expression was comparable to normal control (F3). **(G,H)** Egfr-Em expression was rarely found in CD4^{+} or CD8a^{+} T cells in control colon or in colon after 7 days of DSS treatment.

Move S1 (related to Figure 1)

Internalization of Egfr-Em with EGF upon EGF administration. Rhodamine-labeled EGF (red) was added to the primary ASC cultures generated from *Egfr*$^{Em/Em}$ mice. Internalization of Egfr-Em (green) with Rhodamine-EGF (red) along the phalloidin-labeled microtubules (magenta) was observed upon ligand treatment. Membrane ruffling was detected in some of these cells.

Supplemental Experimental Procedures

Generation of *Egfr*^{Em} mouse

The sgRNA targeting *Egfr* exon 28 (target sequence: sequence AAATGCAGAGTACCTACGGG) was designed according to previous method (Ran et al., 2013). A pair of oligos (fwd: CACCGAAATGCAGAGTACCTACGGG, rev: AAACCCCGTAGGTACTCTGCATTTC) were annealed and ligated to vector pX459 to give rise to pX459-mEgfr-ex28 according to published method (Ran et al., 2013). To test the efficiency of sgRNA-mediated cleavage, IMCD3 cells were transfected with pX459-mEgfr-ex28 in suspension with Lipofectamine 2000. Following 1-1.5 microgram/ml puromycin selection for 1-2 days, total DNA from surviving cells were harvested with Wizard Genomic DNA Purification Kit (Promega). A total of 200 ng genomic DNA was used as template for Surveyor assay with the following primers (fwd: CTTGCTGAGGACACTTGCAG, rev: CCTCACCATGAGGCAAACTTC). The cleavage efficiencies were assessed by measuring the ratio of cleaved product (0.45 kp and 0.35 kb bands) and uncut product (0.8 kb band). To generate the donor construct, a 3 kb 5' flanking fragment, and a 2.5 kb 3' flanking fragment were PCR amplified from genomic DNA isolated from ES cell line of 129/Sv and C57BL/6 hybrid background, and ligated to the cassette with *Egfr* exon 28 fused to Emerald and V5 tag coding sequence before the stop codon. The pX459-mEgfr-ex28 cognate sequences were altered by synonymous point mutations. All constructs were sequenced to verify correct sequences. To generated *Egfr*^{Em} knock-in allele, oocytes from hormone primed and superovulated C57BL/6J mice were collected, and a mixture of 2 ng/microliter pX459-mEgfr-ex28, and 3 ng/microliter donor plasmid was injected into pronuclei. The embryos were transferred into pseudopregnant ICR mice. Potential founders were identified by PCR genotyping (Figure 1A; primers in supplemental materials), and each was crossed to identify germ line transmission. One correctly targeted founder was obtained from a total of seventeen mice that underwent pronuclear injection.

Mice

Egfr$^{tm1(EmeraldV5)Rjc}$ (*Egfr*^{Em}*;* above), *Lrig1*$^{tm1.1(cre/ERT)Rjc}$ (*Lrig1*^{CreERT2}) (Powell et al., 2012), *Apc*^{tm1Tno} (*Apc*^{fl}) (Shibata et al., 1997) were used, and all animals were PCR-genotyped. Animal handling was under protocols approved by Vanderbilt University Medical Center Institutional Animal Care and Use Committee. For tamoxifen induction, *Lrig1*$^{CreERT2/+}$*;Apc*$^{fl/+}$ mice aged 6-8 weeks were injected intraperitoneally with 3 doses of tamoxifen dissolved in corn oil at 2 mg (1 dose per day for 3 consecutive days). For ligand administration *in vivo*, recombinant hEGF (Peprotech, 1 μg per gram body weight) or recombinant hAREG (R&D, 1.87 μg per gram body weight) was injected intraperitoneally. In DSS experiments, mice were provided with water containing 2.5% DSS (Affymatrix) for 7 days, and tissues were harvested.

Cell harvest and primary culture of ASC, intestinal organoids, and neuroblasts

The ASC were prepared as described (Bunnell et al., 2008). In short, the inguinal fat pads were harvested, washed in PBS, minced, digested with 0.1% collagenase (Sigma), and plated and cultured in 20% fetal bovine serum at 37^{o}C in 5% CO_2. For intestinal organoids, crypts were isolated as described (Powell et al., 2012), seeded in Matrigel (BD Biosciences), and cultured in organoid medium (IntestiCult^{TM}). For activation of EGFR signaling, recombinant mEGF (R&D) was used to treat ASC (50 ng/mL) and organoids (200 ng/mL).
For neurosphere culture, the V-SVZ region was micro-dissected from perinatal *Egfr*^{Em} animals, pooled, dissociated (using NeuroCult^{TM} Enzyme Dissociation for Adult CNS Tissue), and maintained in NeuroCult^{TM} NS-A proliferation medium supplemented with 20 ng/ml mEGF and 20 ng/ml hbFGF (Stemcell Technologies). Dissociated cells were maintained on non-adherent sterile petri dishes and half of the media volume was changed every 48 hours. When spheres were between about 100-150 μm in diameter, they were seeded on poly-D-lysine and laminin-coated coverslips in a 24-well plate in EGF- and FGF-free Neurobasal medium supplemented with L-glutamine, 1% FBS, and B27. Cells were formalin-fixed at various time points.

Tissue fixation and immunohistochemistry

Tissues were dissected, fixed (in 4% PFA, 2-4 hours) and processed into cryo blocks according to standard procedures. In short, sections were incubated with primary antibodies at 4^{o}C overnight, followed by short PBS washes and secondary antibodies at room temperature for 2 hours. To prepare wholemount immunostaining of the brain, mouse brains were dissected and processed as described (Doetsch et al., 1999). Briefly, brains were fixed overnight in 4% paraformaldehyde and blocked for 48 hours in 10% normal goat serum with 0.05% Triton-X100 at 4^{o}C. Primary antibodies were incubated at 4^{o}C for 48 hours, followed by secondary antibodies at 4^{o}C overnight. The lateral face of the ventricles was then dissected and mounted in Mowiol for *en* face visualization. Primary antibodies used for immunostaining: Phalloidin (ThermoFisher, 1:1000), E-cadherin (BD science, 1000), GFP (rabbit primary, ThermoFisher, 1:500), GFP (chicken primary, Abcam, 1:500), Pax6 (Covance, 1:500), Tbr2 (Millipore, 1:500), Pitx2 (Capar Science, 1:1000), DCX (Cell Signaling, 1:1000), Lamp1 (Abcam, 1:200), EEA1 (Abcam, 1:200), cKit (Millipore, 1:250), pEgfr (1068Y, Abcam, 1:1000), Lrig1 (R&D, 1:100), β-catenin (BD Bioscience 1:1000), Areg (NeoMarkers, 1:100, with Tyramide signal amplification), F4/80 (eBioscience, 1:100), SMA (Sigma, 1:500), CD4 (eBioscience, 1:100), and CD8a (eBioscience, 1:100). For Tyramide signal amplification, after incubation with primary antibodies, sections were washed with PBS, incubated in biotinylated secondary antibodies (Vector Lab, 1:500), incubated with Avidin/Biotin complex (Vector Lab, per instruction), and incubated with fluorophore-conjugated Tyramide (Perkin Elmer, 1:400). Images were taken using a Nikon A1R or an Olympus FV-1000 confocal microscope. Data analysis, processing and presentation were performed using Image J and Adobe Photoshop (CS6).

Cell lysis and immunoblotting

Lysis buffer, preparation of lysates, and immunoblotting was performed as previously described (Singh et al., 2015). Specifically, intestinal crypt/villus and colonic crypt lysates, crypts and/or villi were isolated from small intestines or colons (Powell et al., 2012), followed by general preparation steps. For lysates from liver and brain, small fragments from the liver or the brain were sonicated in the lysis buffer contains, followed by general preparation steps. Primary antibodies used for immunoblotting: Egfr (EP38Y, Abcam, 1:500), GFP (ThermoFisher, 1:500), pEgfr (1068Y, Abcam 1:1000), pAkt (Cell Signaling, 1:1000), Akt (Cell Signaling, 1:1000), pErk1/2 (Cell Signaling, 1:1000), Erk1/2 (Cell Signaling, 1:1000), Egfr (1:1000), and α-tubulin (Cal Biochem, 1:4000). Detailed information for primary antibodies used in this work are listed in the Resource Table.

Densitometric quantification of Egfr in cycloheximide chase assay

Data were collected from three independent experiments performed in triplicate. For each time point, the intensity of Egfr from immunoblotting was determined by the "integrated density" function of ImageJ and normalized to the intensity of Vinculin from the same sample. The percentage of the Egfr intensity for each time point was compared to that at time 0 minute. Data represent percentage of Egfr intensity of three independent experiments (mean ± SEM) compared with that at time 0 minute. No significant difference was found by a Student's t-test.

Quantification of membranous fraction of Egfr

Quantification of the plasma fraction of Egfr immunofluorescence was analyzed using ImageJ software. Na^+/K^+ ATPase immunofluorescence expressed at the plasma membrane was used as control. Signal and background of images for Egfr-Em and Na^+/K^+ ATPase obtained by confocal microscopy was separated by 'threshold' function in ImageJ. Pixels with both Egfr-Em and Na^+/K^+ ATPase signals were determined by 'image calculator' function in ImageJ. Then plasma membrane fraction of Egfr-Em was calculated by 'measure' function in ImageJ. Differences in the normalized intensity of Egfr-Em between EGF and AREG treatment was subjected to a Student's t-test.

Quantification of Egfr-Em expression versus pEgfr expression in normal crypts and adenomas

Area of normal crypts and adenomas were selected manually in ImageJ. Signal and background of images for Egfr-Em and pEgfr obtained by confocal microscopy was separated by 'threshold' function. Pixels with Egfr-Em/pEgfr co-expression and total pEgfr expression were determined by measuring the integrated density function. Areas of 68 randomly selected normal crypts and areas of 21 randomly selected adenomas were calculated and subjected to a Student's t-test.

Resources Table

REAGENT or RESOURCE	SOURCE	IDENTIFIER
Antibodies		
Mouse monoclonal anti-E-cadherin	BD Bioscience	#BDB610181
Rabbit polyclonal GFP	ThermoFisher	#A-11122
Chicken polyclonal GFP	Abcam	#ab13970
Rabbit polyclonal Pax6	Covance	#PRB-278P
Rabbit polyclonal Tbr2	Millipore	#ab15894
Rabbit polyclonal Pitx2	Capra Science	#PA1020-100
Rabbit polyclonal DCX	Cell Signaling	#4604
Rat polyclonal Lamp1	Abcam	#ab25245
Rabbit polyclonal EEA1	Abcam	#ab2900
Rat monoclonal cKit	Abcam	#ab5506
Goat polyclonal Lrig1	R&D	#AF3688
Mouse monoclonal β-catenin	BD Bioscience	#BDB610154
Rabbit polyclonal AREG	ThermoFisher	#RB257P0
Rat monoclonal F4/80	eBioscience	Clone BM8
SMA	Sigma	C6198
Rat monoclonal CD4	eBioscience	Clone 4SM95
Rat monoclonal CD8a	eBioscience	Clone 4SM16
Rabbit monoclonal Egfr (Phospho-Y1068)	Abcam	#ab32430
Rabbit polyclonal Egfr (EP38Y)	Abcam	#ab52894
Rabbit polyclonal Egfr	Abcam	#ab15669
Rabbit polyclonal Phospho-Akt (Ser473)	Cell Signaling	9271S
Rabbit polyclonal Akt	Cell Signaling	9272S
Rabbit polyclonal Phospho-p44/p42 MAPK	Cell Signaling	9101S
Rabbit polyclonal Erk1/2	Cell Signaling	9102S
Mouse monoclonal α-tubulin (DM1A)	Millipore	CP06
Biological Samples		
Mouse genomic DNA from 129/Sv and C57BL/6 hybrid background	Vanderbilt University Transgenic Mouse/ES Cell Shared Resource	N/A
Oocytes from C57BL/6J	Vanderbilt University Transgenic Mouse/ES Cell Shared Resource	N/A
Chemicals, Peptides, and Recombinant Proteins		
Recombinant mouse EGF	Peprotech	315-09
Recombinant mouse EGF	R&D	2028-EG-200
Recombinant human AREG	R&D	262-AR-100
EGF, rhodamine-conjugated	ThermoFisher	E3481
Critical Commercial Assays		
Cytoskeleton Kit (SiR-Tubulin)	Cytoskeleton Inc	#CY-SC006
Surveyor Mutation Detection Kits	Integrated DNA Technologies	706025
Experimental Models: Organisms/Strains		
Mouse: *Egfr*^{Em}	This paper	N/A
Mouse: *Lrig1*^{CreER}: *Lrig1*$^{tm1.1(cre/ERT)Rjc}$	Powell et al., 2012	JAX: 018418
Mouse: *Apc*^{fl}: *Apc*^{tm1Tno}	Shibata et al., 1997	N/A

Recombinant DNA		
Plasmid: pX459	Ran et al., *Nat Protoc.* (2013) 8, 2281-2308.	Addgene Plasmid # 62988
Plasmid: pX459-mEgfr-ex28	This paper	N/A
Plasmid: pUC57-Egfr-Emerald-V5	This paper	N/A
Plasmid: pUC57-Egfr-Emerald-V5-long donor	This paper	N/A
Sequence-Based Reagents		
Primers: $Egfr^{Em}$ and $Egfr^{wt}$ genotyping: Common forward CCACAGCTGAAAATGCAGAG $Egfr^{Em}$ reverse TGGTGCAGATGAACTTCAGG $Egfr^{wt}$ reverse CCTCACCATGAGGCAAACTT	This paper	N/A
Primer: pX459-mEgfr-ex28 Forward: CACCGAAATGCAGAGTACCTACGGG	This paper	N/A
Primer: pX459-mEgfr-ex28 Reverse: AAACCCCGTAGGTACTCTGCATTTC	This paper	N/A
Primer: surveyor assay primer Forward: CTTGCTGAGGACACTTGCAG	This paper	N/A
Primer: surveyor assay primer Reverse: CCTCACCATGAGGCAAACTTC	This paper	N/A
Primer: founder identification primer Forward: CAGTGGGCAACCCTGAGTATC	This paper	N/A
Primer: founder identification primer Reverse: TGCTCAGGTAGTGGTTGTCGGG	This paper	N/A
Primer: left arm primer Forward: CAGTGAATTCGAGCTCGGTACAGATGCTGATAGCCG CCCAAAGTTCCG	This paper	N/A
Primer: left arm primer Reverse: CTGCAAGTGTCCTCAGCAAGACAACCG	This paper	N/A
Primer: Emerald primer Forward: CTTGCTGAGGACACTTGCAG	This paper	N/A
Primer: Emerald primer Reverse: GATGTACCTTCAACTTCCCAAAGTGC	This paper	N/A
Primer: right arm primer Forward: GCACTTTGGGAAGTTGAAGGTACATCAATTGATCTTC G	This paper	N/A
Primer: right arm primer Reverse: CGCCAAGCTTGCATGCAGGCCTGTGGGCTGAAAGGC AGTTAGTAGAAAGATGC	This paper	N/A
Software and Algorithms		
Image J	NIH	N/A
Photoshop CS6 or CC	Adobe	CS6, CC
Other		
Wizard Genomic DNA Purification Kit	Promega	A1120
Gibson Assembly Master Mix	New England BioLabs	E2611S
QIAprep Spin Miniprep Kit	Qiagen	27106
PfuUltra II Fusion HS DNA Polymerase	Agilent Technologies	600670

Supplemental References

Bunnell, B.A., Flaat, M., Gagliardi, C., Patel, B., and Ripoll, C. (2008). Adipose-derived stem cells: isolation, expansion and differentiation. Methods *45*, 115-120.
Doetsch, F., Caille, I., Lim, D.A., Garcia-Verdugo, J.M., and Alvarez-Buylla, A. (1999). Subventricular zone astrocytes are neural stem cells in the adult mammalian brain. Cell *97*, 703-716.
Powell, A.E., Wang, Y., Li, Y., Poulin, E.J., Means, A.L., Washington, M.K., Higginbotham, J.N., Juchheim, A., Prasad, N., Levy, S.E.*, et al.* (2012). The pan-ErbB negative regulator Lrig1 is an intestinal stem cell marker that functions as a tumor suppressor. Cell *149*, 146-158.
Ran, F.A., Hsu, P.D., Wright, J., Agarwala, V., Scott, D.A., and Zhang, F. (2013). Genome engineering using the CRISPR-Cas9 system. Nature protocols *8*, 2281-2308.
Shibata, H., Toyama, K., Shioya, H., Ito, M., Hirota, M., Hasegawa, S., Matsumoto, H., Takano, H., Akiyama, T., Toyoshima, K.*, et al.* (1997). Rapid colorectal adenoma formation initiated by conditional targeting of the Apc gene. Science *278*, 120-123.
Singh, B., Bogatcheva, G., Starchenko, A., Sinnaeve, J., Lapierre, L.A., Williams, J.A., Goldenring, J.R., and Coffey, R.J. (2015). Induction of lateral lumens through disruption of a monoleucine-based basolateral-sorting motif in betacellulin. Journal of cell science *128*, 3444-3455.